Selective Nerve Cuff Stimulation Strategies for Prolonging Muscle Output

Kristen T. Gelenitis, Brian M. Sanner, Ronald J. Triolo, and Dustin J. Tyler

***Abstract*—Neural stimulation systems are often limited by rapid muscle fatigue. Selective nerve cuff electrodes can target independent yet synergistic motor unit pools (MUPs), which can be used in duty-cycle reducing stimulation paradigms to prolong joint moment output. *Objective:* This study investigates waveform parameters within moment-prolonging paradigms and determines strategies for their optimal implementation. *Methods:* Composite flat-interface nerve cuff electrodes (C-FINEs) were chronically implanted on feline proximal sciatic nerves. Cyclic stimulation tests determined effects of stimulation period and duty cycle in different MUP types. Ideal parameters were then used in duty-cycle reducing carousel stimulation. Time to 50% reduction in moment (T50), moment overshoot, and moment ripple were determined for constant, open-loop carousel, and moment feedback-controlled closed-loop carousel stimulation. *Results:* A stimulation period of 1 s best maintained joint moment for all MUPs. Low (25%) duty cycles consistently improved joint moment maintenance, though allowable duty cycle varied among MUPs by gross muscle and fiber type. Both open- and closed-loop carousel stimulation significantly increased T50 over constant stimulation. Closed-loop carousel significantly decreased moment overshoot over the other conditions, and significantly decreased moment ripple compared with open-loop stimulation. *Conclusion:* Selectivity-enabled carousel stimulation prolongs joint moment over conventional constant stimulation. Appropriate waveform parameters can be quickly determined for individual MUPs and stimulation can be controlled for additional performance improvements with this paradigm. *Significance:* Providing prolonged, stable joint moment and muscle output to recipients of motor neuroprostheses will improve clinical outcomes, increase independence, and positively impact quality of life.**

***Index Terms*—Neural engineering, fatigue.**

Manuscript received April 28, 2019; revised July 19, 2019; accepted August 18, 2019. Date of publication August 26, 2019; date of current version April 21, 2020. This work was supported in part by the National Institutes of Health (#5-R01-EB001889-11 and #5-T32-EB004314-18) and in part by resources and use of facilities at the Louis Stokes VA Medical Center. *(Corresponding author: Kristen T. Gelenitis.)*

K. T. Gelenitis is with the Department of Biomedical Engineering, Case Western Reserve University, Cleveland, OH 44106 USA, and also with Louis Stokes VA Medical Center, Cleveland, OH 44106 USA (e-mail: kxg277@case.edu).

R. J. Triolo and D. J. Tyler are with the Department of Biomedical Engineering, Case Western Reserve University, and also with Louis Stokes VA Medical Center.

B. M. Sanner is with the Department of Biomedical Engineering, Case Western Reserve University.

Digital Object Identifier 10.1109/TBME.2019.2937061

I. Introduction

STIMULATION for coordinated contraction of paralyzed muscles enables individuals with spinal cord injury and other neuromuscular disorders to regain lost functions. However, contractions generated by neural stimulation are often subject to fatigue with different muscles fatiguing at different rates. The decline in joint moment output and changes in muscle coordination with fatigue can ultimately limit the benefits and independence that motor system neural prostheses offer.

One reason commonly cited for this rapid fatigue is the reversal of physiologic motor unit recruitment order with extracellular stimulation [1], [2]. Large, fast fatigable fibers fire at lower charge thresholds than small, slowly fatiguing fibers under extracellular stimulation. This recruitment order is the reverse of physiologic recruitment of slow to fast fibers [3], [4], and it results in swift fatigue of the strongest muscle fibers. Attempts to restore the natural recruitment order have been made with complex electrode arrays that altered the shape of the extracellular field [5] or varied stimulus pulse shapes and amplitudes [6], [7]. Though such techniques have shown that small, slowly fatiguing fibers fire at lower thresholds in acute animal studies, they have not been implemented in humans due to the complexity of generating the waveforms required with currently available implant technologies. Furthermore, subsequent literature has suggested that extracellular stimulation does not simply reverse the recruitment order but rather recruits in a "non-selective, spatially-fixed" pattern, independent of fiber size or type [8]. Even with the correct recruitment order, the same fibers would be repeatedly activated and likely lead to fatigue. Therefore, reversing the order is less of an imperative for reducing fatigue than finding parameters that delay fatigue of each motor unit regardless of when they are recruited.

Extracellular stimulation also causes synchronous firing of all activated fibers as opposed to the asynchronous, stochastic firing that occurs under physiologic conditions [8]. Asynchronous firing allows for each individual motor unit to have a lower firing frequency, as other motor units firing at different frequencies or offsets in time will maintain overall muscle tone, creating a highly coordinated contraction. Multiple research groups have investigated interleaved stimulation as a way to more closely mimic the physiologic asynchrony with extracellular stimulation [9]–[11]. In interleaved stimulation, the total desired firing frequency is divided and interspersed among independent, synergistic motor unit populations. This creates unfused contractions on individual motor units that sum together for full tetany

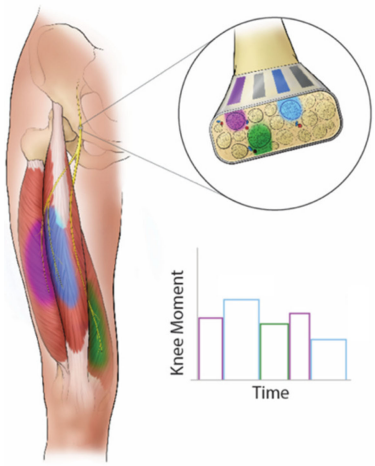

Fig. 1. An example of carousel stimulation through a selective nerve cuff with three independent synergistic motor unit pools. Stimulating through one nerve cuff contact at a time causes some motor units to create a joint moment while inactive motor units rest and recover.

at the originally desired frequency. This approach moderately improves the maintenance of joint moment over constant stimulation [9]–[11]. However, interleaved stimulation consistently results in a decrease in maximum achievable force [11], which may limit its utility during functional maneuvers that require large muscle forces and joint torques, such as standing, transfers, or stepping.

Conventional motor system neural prostheses generally employ non-selective stimulation. That is, they cause a constant contraction of many motor units within a targeted muscle and therefore quickly fatigue many fibers at once. Poor selectivity has been cited as a major limitation of surface [12], [13] and intramuscular [14] approaches alike. Selective multi-contact nerve cuff electrodes have been designed and verified chronically *in vivo* to activate independent yet synergistic motor unit pools (MUPs) from a common location on a nerve trunk [15]–[20]. Advanced stimulation paradigms that utilize this selectivity have been proposed to prolong moment output with neural stimulation. Such paradigms alternate activation of multiple synergistic yet independent motor unit pools, allowing some fibers to rest and recover while others maintain the required joint moment to complete a functional task. Implementation of one such a paradigm is carousel stimulation through a selective nerve cuff electrode (Figure 1).

Advanced paradigms such as carousel stimulation introduce waveform parameters that may alter their effectiveness. Duty cycle (the relative ratio of "on" to "off" times of a given set of motor units) and stimulation period (the absolute duration of a single "on" time) are important factors to be considered for optimal implementation. Optimal values for these parameters may also vary among motor unit pools (MUPs) involved in the paradigm. To narrow the parameter space and expedite the selection of MUPs associated with these paradigms prior to human implementation, this work explores their relative effects in a chronic feline model with multi-contact nerve cuff electrodes implanted on the sciatic nerve. Furthermore, maintaining balanced output

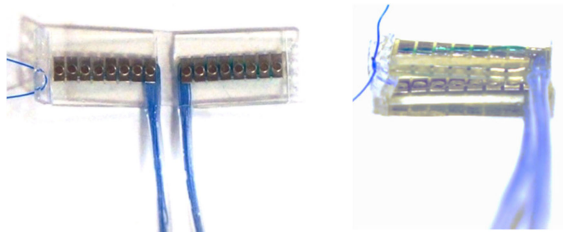

Fig. 2. The C-FINE electrode. A 16-channel C-FINE electrode in open (left) and closed (right) conformations.

from each MUP, despite different degrees of potentiation and fatigue, is also necessary for optimal implementation of these paradigms. This may be done by adjusting the stimulation current through each contact during active stimulation periods. The exact current needed to achieve a given joint moment at any time changes based on the muscle fibers' activation histories, making feed-forward, open-loop control challenging after prolonged muscle activation [21], [22]. A closed-loop stimulation system that utilized joint moment feedback was therefore developed to adjust stimulation parameters in real-time for better control of these paradigms.

We tested the following hypotheses:

1. effective, moment-prolonging stimulation waveform parameters differ by muscle and fiber type recruited by each contact on a selective nerve cuff;
2. motor unit pool fatiguability can be identified through twitch contraction time measures and joint moment trajectories;
3. closed-loop control of duty cycle-reducing paradigms will further prolong moment output and increase stability over open-loop stimulation.

II. Methods

A. Multi-Contact Electrode Implantation

All animal procedures were approved by the Institutional Animal Care and Use Committee of the Louis Stokes Cleveland Veteran Affairs Medical Center. Four adult cats were implanted with 16-contact composite flat-interface nerve cuff electrodes (C-FINEs, Ardiem, Inc, PA) bilaterally on the sciatic nerves proximal to the bifurcation for a total of 8 implanted electrode cuffs and 128 independent contacts. The C-FINEs (Figure 2) consist of thin layers of flexible silicone elastomer sandwiching a narrow layer of polyether ether keytone (PEEK) polymer stiffening bar with an array of platinum contacts on the top and bottom of the cuff. This configuration has been shown to gently reshape the nerve into an elongated oval [23] which allows individual contacts along the width of the nerve to selectively access different fascicles with minimal to no effect on nerve health [24], [25].

Isoflurane gas was administered via intubation for anesthesia maintenance, and saline drip was given intravenously. An incision was made on the proximal hindlimb to expose the sciatic nerve. The cuff was secured around the nerve with suture. Leads from each cuff were manipulated into multiple

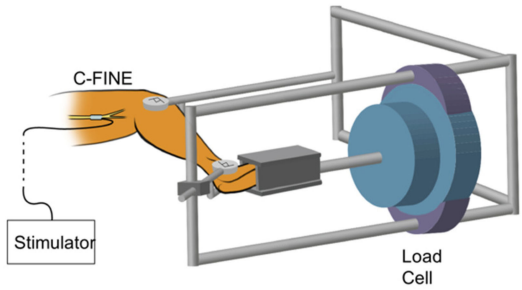

Fig. 3. A schematic of the experimental setup. The hindlimb is fixed in a stereotactic frame with the hip, knee, and ankle joints at 90°. The paw is secured to a metal shoe attached to a 6 degree of freedom load cell, which measures ankle moments produced by C-FINE stimulation.

stress-relief loops before being tunneled cranially to a percutaneous exit site between the scapulae to limit animal access. Each animal was fitted with a vest and collar to further reduce access to the exposed wire when not testing. No lasting adverse physiological or behavioral effects were observed post-implantation in any of the animals due to the implanted electrodes or their leads.

B. Experimental Setup

Each cuff was tested approximately every second week from three weeks post-implantation to the final procedure. This chronic study lasted 24 months from implant of the first animal to explant of the last. During data collection, the hindlimb was fixed in a stereotactic frame as described by Grill *et al.* [20] (Figure 3). The paw was firmly secured to a metal shoe attached to a 6 degree of freedom load cell (JR3 Inc., Woodland, CA). The load cell recorded moments produced about the ankle from charge-balanced, asymmetric cathodic stimulation delivered through the percutaneous leads by a custom computer-controlled external stimulator [26]. Stimulation was controlled by a custom MATLAB Simulink model (MathWorks, Natick, MA) running on an xPC host- target, and post-operative data processing was also conducted via custom MATLAB code.

C. Moment Space Generation

Stimulation thresholds for each contact were determined by injecting low amplitude pulses while manually palpating the muscle. The lowest amplitude that generated a just noticeable contraction at a 100 μs pulse width was used for each contact. Stimulation frequency was always set to 33 Hz, as this was found to be the lowest frequency that reliably induced fused tetanic contractions on all contacts. And, since low frequencies have been shown to reduce fatigue, a higher frequency is a more challenging and informative test [27]. Tetanic recruitment curves were generated by a discrete increasing ramp method [28]. At the chosen pulse amplitude, one-second bursts of stimulation were delivered, separated by five seconds of rest, until the entire stimulator pulse width range, 5 to 255 μs in 10 μs increments, was covered. If a full recruitment curve, from threshold (just noticeable contraction) to saturation (maximal contraction without activating reflexes or spilling over into unwanted muscles), was not produced over this range of pulse durations, the amplitude was increased by 0.1 mA and the recruitment curve was recollected. Moment output at the ankle was averaged over the last 0.25 seconds of each tetanic contraction to obtain steady state values, and data was analyzed in the plantar/dorsiflexion vs. medial/lateral rotation moment space.

D. Determination of Overlap

Pairwise tetanic overlap tests [11] were performed on contacts primarily eliciting plantarflexion in each cuff to determine the potential number of independent yet synergistic motor unit pools for the moment-prolonging paradigms. The stimulating current to generate 50% of the maximal moment of the recruited muscle was delivered in five two-second bursts. This was then repeated for a second contact. Finally, stimulating current was applied to both contacts with a 1 ms delay between pulse trains to eliminate field effects while the second MUP was activated within the refractory period of the first. In the absence of muscle fiber overlap, the moment produced from stimulating both contacts would equal the sum of the moments produced from stimulating the contacts individually. When overlap is present, the moment produced from stimulating both contacts at once is less than the sum of the contacts individually. Percent overlap between two contacts is calculated as the percent deviation of the combined moment from the perfect sum of the two independent moments as described by Yoshida *et al.* [11]. For the purposes of this study, MUPs with less than 30% total overlap were considered suitable for use in duty cycle-reducing paradigms [29].

E. Cyclic Stimulation Protocol

Cyclic stimulation parameters were set to the pulse amplitude and pulse width that activated each motor unit pool at 50% of its plantar flexion recruitment curve on the experimental day. This provided consistency across testing sessions and across contacts. To eliminate confounding effects of muscle potentiation, MUPs were pre-conditioned immediately prior to a cyclic stimulation trial with five two-second tetanic bursts for ten seconds total of potentiating stimulation [30]. This protocol was found to reliably and maximally potentiate most MUPs tested without moving past potentiation and into fatigue (Figure 4, Phase 1).

Following the potentiation phase, five individual muscle twitches were evoked at a rate of one twitch per second with the same 50% stimulation parameters (Figure 4, Phase 2). The averaged post-potentiation twitch responses were used in post-hoc analyses as a method of separating motor unit types. As described by Reinking *et al.* [31], MUPs with twitch contraction times greater than 45 ms were characterized in this study as slow twitch fibers, while those with contraction times less than 45 ms were herein characterized as fast twitch fibers. The fast twitch fiber population was further broken down into pure fast twitch, for those showing only one true peak, and mixed fibers, for those showing an initial fast twitch contraction time followed by a second, slower peak. Though each MUP may contain

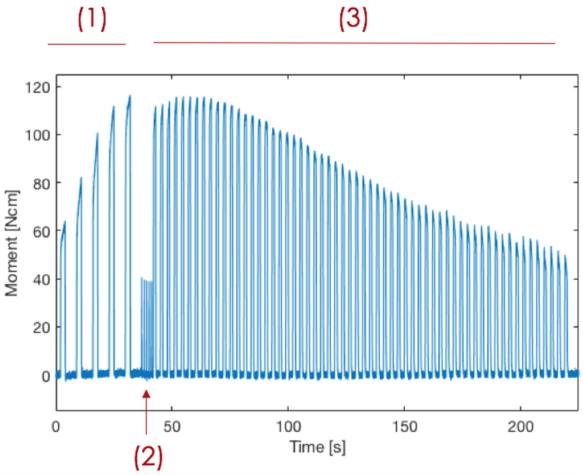

Fig. 4. An example of data from each phase of the cyclic stimulation protocol. The potentiation phase (1), the potentiated twitch response (2), and the cyclic parameter testing phase (3).

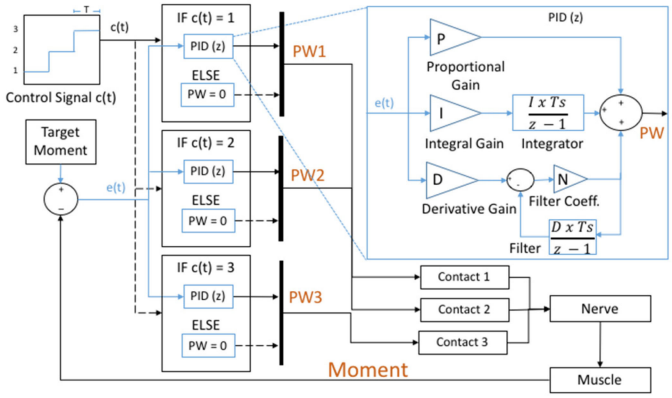

Fig. 5. The closed-loop carousel stimulation scheme. A carousel control signal *c(t)* determines which contact is stimulated through at each timepoint. Independently tuned PID controllers adjust the instantaneous PW sent through the active contact based on real-time joint moment feedback from the load cell. PW is adjusted to minimize the error *e(t)* between target and actual moment output.

multiple fiber types, these classifications represent the predominant fiber type present based on twitch contraction time.

Cyclic stimulation was delivered through a single contact at the pulse width yielding 50% of the maximum recruited moment immediately following the potentiated twitches. To determine the effect of stimulation period, or the length of time a single MUP is activated before allowed to rest, currents were delivered to contacts with active times of one, five, or ten seconds at a 50% duty cycle. To determine the effect of duty cycle on moment output, current was applied to contacts with a stimulation period of one second at 25%, 33%, and 50% duty cycles. Each stimulation period and duty cycle test continued until a total active stimulation time of one minute was reached (Figure 4, Phase 3). Recovery periods of at least 20 minutes were allowed between cyclic stimulation trials on the same experiment day to minimize fatigue effects, and MUPs were briefly stimulated prior to beginning a new fatigue trial to ensure return to within 5% of their initial moment output.

Cyclic stimulation outcome measures included normalized mean moment and normalized mean within-contraction change in moment (i.e., "Delta") over the one minute of active stimulation in Phase 3. The average moment was computed as the mean of the raw moment output during all active contractions (rest period baseline moments were ignored). Delta was calculated for each individual contraction as the variation, or range, in moment output within that contraction. Average delta for a trial was computed as the mean of the individual contraction deltas from that trial. Both average moment and average delta were normalized to the maximum moment achieved in Phase 3 for each trial. Average moment provides a measure of how well each test condition maintains maximum moment output, while average delta provides a measure of how stable this evoked moment output is within each stimulation period. Optimal stimulation period and duty cycles were chosen as those that resulted in the highest average moment output while producing the lowest average delta.

F. Carousel Stimulation Protocol

Open and closed-loop carousel trials in which stimulation is sent through multiple contacts sequentially demonstrated effectiveness of the optimal stimulation period and duty cycles found with cyclic stimulation. In open loop trials, stimulation parameters for each MUP were chosen based on each MUP's recruitment curve such that moment output should reach 50% of the weakest MUP's maximal moment. These parameters were set at the beginning and held constant throughout the fatiguing carousel trial.

Closed-loop experiments utilized moment feedback from the load cell to continuously adjust pulse widths independently on each contact (Figure 5) throughout the trial. A repeating carousel control signal *c(t)* determined which contact was stimulated through at each time point. This carousel signal held one contact active for one stimulation period (T). The signal then switched to deliver current through a different contact for the next period. This was repeated for each involved contact and cycled continuously throughout the trial. There was no ramping up or down of pulse widths when contacts were switched such that only one MUP was active at a time. Other contacts received PA and PW values of zero to avoid field interactions and ensure independence of the MUPs activated. An error signal *e(t)* produced from differences between the target moment and actual load cell-recorded moment drove the active contact's PID controller. Discrete PID controllers use proportional, integral, and derivative gains to adjust controller output *y(z)* at each time step until the error is minimized according to the control law:

$$y(z) = P + I\alpha(z) + D\left[\frac{N}{1 + N\alpha(z)}\right] \tag{1}$$

where P = proportional gain, I = integral gain, D = derivative gain, N = derivative filter coefficient, and

$$\alpha(z) = \frac{T_s}{z - 1} \tag{2}$$

In this study, the output of the PID controller $y(z)$ is the PW provided directly to the active contact. PID gain constants were manually tuned on each contact individually prior to full carousel controller implementation. Initial PID output values were set to the PWs predicted to produce 50% of the weakest MUP's maximal moment based on each MUP's recruitment curve, as in open-loop trials.

Carousel stimulation outcome measures include average moment ripple index ($\overline{Ri}$), moment overshoot, and T50. Moment ripple index (Ri) is calculated as the ratio of the peak-to-peak moment output to the average moment output over one full cycle through each contact in the paradigm. Mean moment ripple index ($\overline{Ri}$) is taken as the mean of moment ripple indices over all cycles of the paradigm for the duration of the trial. Moment overshoot is determined as the maximum deviation of the average moment from the desired moment and is expressed as a percentage of the desired moment. T50 is defined as the time at which the raw moment output declines to 50% of the desired moment. Raw moment is used instead of average moment for T50 values to fairly reflect the effect of ripple in carousel trials. Reduced moment ripple, decreased moment overshoot, and increased T50 are indicators of superior implementation of these paradigms and prolonged, stable moment output.

G. Statistical Analyses

Statistical comparisons of all outcome measures were performed using one-way ANOVAs with the Bonferroni correction method for multiple comparisons. These analyses test the null hypotheses that the pairwise difference between data from different conditions has a mean equal to zero. Significance levels are reported based on the highest p-value obtained from the MATLAB function *multcompare*.

III. Results

A. Nerve Cuff Selectivity

Stimulation through each 16-contact C-FINE selectively activated all major muscles innervated by the feline proximal sciatic nerve at all follow-up time points. Figure 6 shows the moment space trajectories produced by stimulating through each of the contacts on a single cuff. Moment space trajectories collected during this study were compared with data obtained by from several studies [15], [19], [23], [32] that show the trajectories obtained from activating the medial gastrocnemius (MG), lateral gastrocnemius (LG), soleus (SOL), tibialis posterior (TP), and common peroneal (CP) branches individually. Based on these moment space trajectories, each contact was classified by the muscle predominantly activated. Each of the major branches were activated through at least one selective contact per cuff.

Pairwise overlap testing of plantarflexion contacts further established nerve cuff selectivity. Examples of high and low overlapping contact pairs are shown in Figure 7. Pairwise overlap testing revealed at least two plantarflexing contacts per cuff with less than 30% overlap at a 50% activation level at all time points tested. The variable "c" was chosen to represent the number of contacts on a single cuff with a synergistic output and less

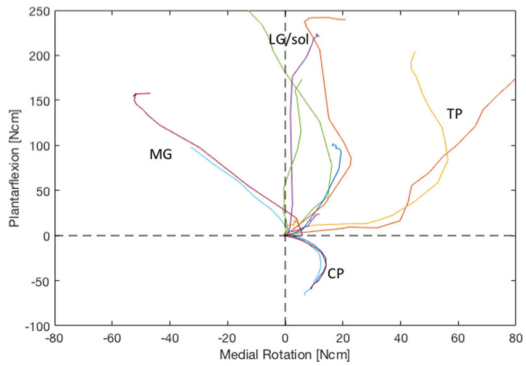

Fig. 6. Sample moment space trajectories from the present study and their muscle classifications (MG, LG/Sol, TP, CP) as determined by comparison with Leventhal *et al.* [19]. Each colored line shows the trajectory achieved through stimulating a different cuff contact in this study. Note that there are five selective trajectories and at least two contacts that produce each trajectory. These contacts are further analyzed for overlap to see if they are recruiting the same MUPs or functionally redundant but unique MUPs that can be used for fatigue reduction.

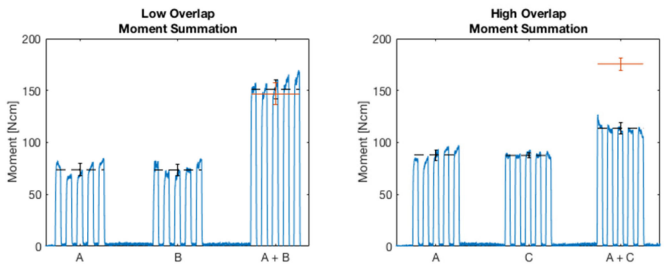

Fig. 7. Plantarflexion moment summation of low (%OL = 1.4) and high (%OL = 48) overlapping contact pairs. The difference in actual moment summation from ideal summation (solid orange) shows extent of fiber overlap. Error bars signify standard deviation.

than 30% total overlap. Groups of $c = 2$, $c = 3$, and $c = 4$ low overlapping contacts were identified at various testing sessions throughout the study. The C-FINE is consistently and reliably able to target multiple independent plantar flexor fiber groups through stimulation of separate contacts within the same nerve cuff. This enables the reduction of duty cycle in advanced stimulation paradigms. When duty cycle is held constant for each MUP, it is equal to the inverse of the number of independent MUPs involved. Duty cycles of 50% ($c = 2$), 33% ($c = 3$), and 25% ($c = 4$) were thus tested in the cyclic stimulation experiments through 33 randomly selected contacts across the 8 nerve cuffs.

B. Motor Unit Type Identification

The potentiated twitch portion of the stimulation protocol resulted in three characteristic twitch contraction profiles (Figure 8). Eleven fast and 1 slow twitch MUPs were identified from the 12 contacts randomly chosen for stimulation period testing. Eighteen fast, 10 mixed, and 5 slow twitch MUPs were identified within the 33 contacts randomly chosen for duty cycle parameter testing.

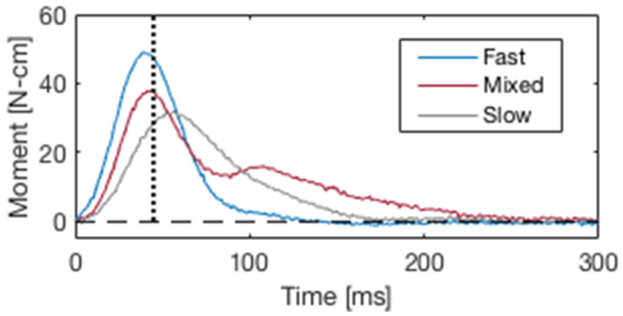

Fig. 8. Examples of the three twitch profiles used to classify MUPs into fiber type categories. Typical fast, mixed, and slow twitch profiles. A twitch contraction time cutoff of 45 ms (vertical dotted line) is used to classify MUPs as fast or slow [31]. Presence of absence of a second peak is used to classify mixed and pure fast fibers respectively.

C. Effect of Stimulation Period

Cyclic stimulation at a 50% duty cycle with periods of one, five, and ten seconds were delivered to twelve randomly chosen contacts across the four cats. Average moment output over 1 minute of active stimulation time and average change in moment within a single contraction (Delta) for each condition are shown in Figure 9. Average moments and deltas are normalized to the maximum moment output of each trial.

Significant differences ($p < 0.015$) in mean moment output were found between periods of one and five seconds and periods of one and ten seconds, with a stimulation period of one second maintaining higher moments for the same amount of contraction time. Similarly, the T = 1 second condition showed significantly ($p < 0.015$) less mean moment decline within muscle contractions than the longer stimulation periods. Following this trend, shorter stimulation periods of T = 0.5 and T = 0.3 were briefly investigated, but did not allow enough time for full relaxation of the muscle between active periods at the 50% duty cycle. Thus, T = 1 second served as the lower bound. As T = 1 second was found superior than longer periods for all tested contacts regardless of muscle or twitch contraction time in both mean moment and mean delta, it was used in all subsequent duty cycle testing.

D. Effect of Duty Cycle

Cyclic stimulation trials with 50%, 33%, and 25% duty cycles were conducted with a stimulation period of T = 1 second. Tested duty cycles were chosen based on the minimum number of MUPs required for implementation of advanced paradigms ($c = 2, 50\%$) and the highest number independent plantar flexion pools consistently identified within a single 16-contact nerve cuff ($c = 4, 25\%$). Post-potentiation mean moment output over one minute of active stimulation were determined at each duty cycle (Figure 10).

Significant differences ($p < 0.01$) in moment maintenance were found between each duty cycle for all contacts tested when pooled. As expected, lower duty cycles that enable longer rest periods before active stimulation showed significantly higher

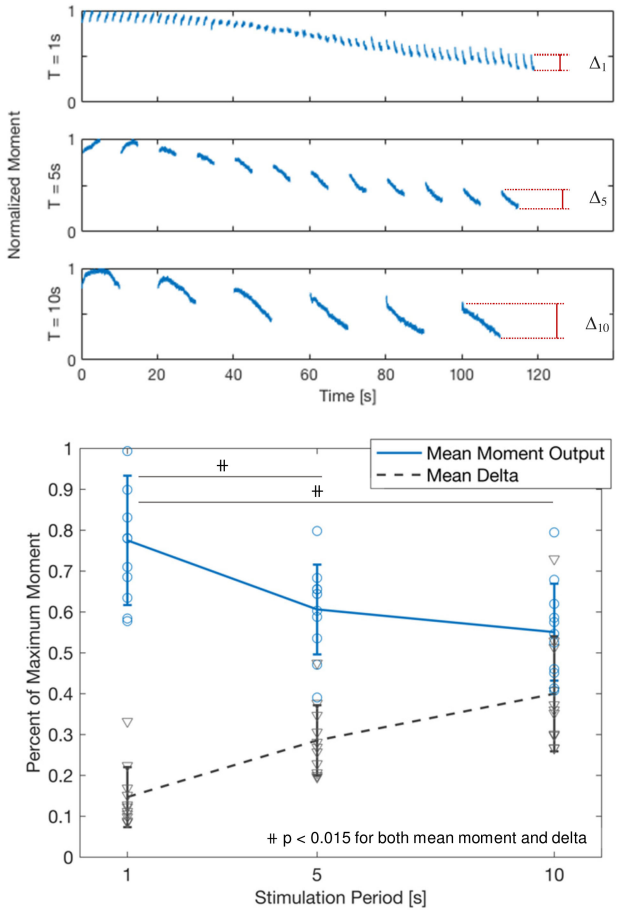

Fig. 9. (Top) Example data showing normalized moment output from cyclic stimulation trials on the same MUP with different stimulation periods. Delta, the within-contraction change in moment, is indicated for the final contraction of each period by the symbol Δ_T. (Bottom) Mean moments (solid blue) and mean deltas (dashed grey) for stimulation periods of T = 1, 5, and 10 seconds after 1 minute of active stimulation at a 50% duty cycle. Each data point represents the mean value for a single trial. Error bars indicate standard deviation. A period of T = 1 second maintains significantly ($p < 0.015$) higher moments with significantly less within-contraction moment decline.

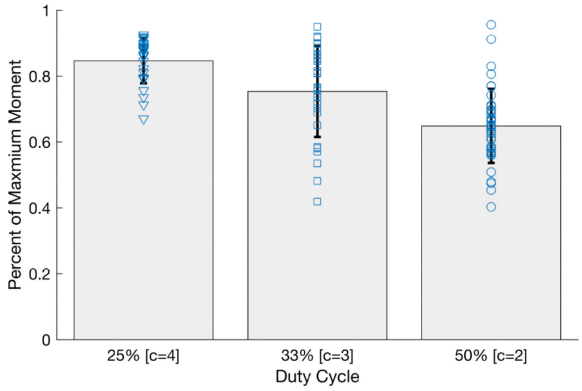

Fig. 10. The normalized mean moment outputs over 1 minute of active stimulation for 33 MUPs tested at each duty cycle. Error bars signify standard deviation. Lower duty cycles resulted in significantly ($p < 0.01$) greater moment maintenance.

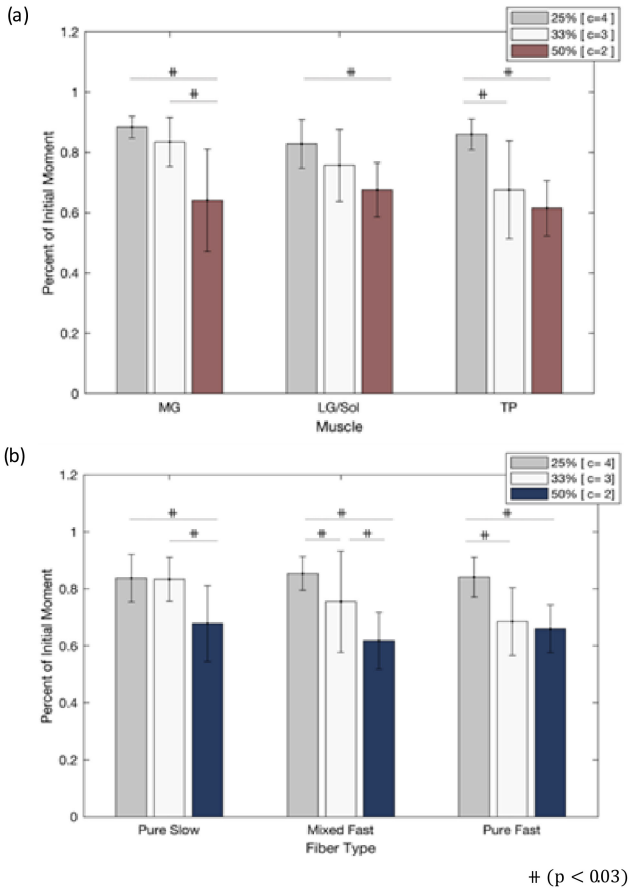

Fig. 11. Mean moment output (a) by predicted muscle and (b) by fiber type at different duty cycles. Error bars indicate standard deviation. Duty cycles sufficient to maintain significantly higher moment outputs after the same active stimulation time vary among muscles and fiber types.

mean moment output after the same total contraction time. Large standard deviations, especially in the 33% duty cycle condition, prompted further analyses to determine ways to quickly distinguish motor unit pools that can handle higher burdens from those that cannot.

When separated by predicted muscle based on moment space trajectory (Figure 11a), key significant ($p < 0.03$) differences among muscles were determined. MG motor units show significantly less moment output at 50% than both 33% and 25% duty cycles. LG/sol motor units showed significantly lower moments at 50% than 25% duty cycles only; the 33% condition did not show significant differences from either of the other conditions. TP motor unit moments were significantly lower at both 50% and 33% than at 25%. The variation in significant differences found here suggests that allowable duty cycle for best maintenance of joint moment differs on a muscle by muscle basis. MG fibers could handle a higher 33% duty cycle while the other muscles could not. This indicates contacts that elicit MG contraction can be interspersed more frequently within a paradigm than those that recruit LG/sol and TP muscle fibers, which show large moment decline at any burden higher than 25%.

The same duty cycle results broken down by twitch contraction time (Figure 11b) also indicated differences in optimal duty cycle selection. Within each duty cycle, only the 33% condition showed significant ($p < 0.03$) differences between fiber type groupings. MUPs classified as purely slow twitch maintained significantly higher average moments at 33% than those classified as purely fast or mixed twitch. The slow group showed no significant difference between 25% and 33% duty cycles, which were both significantly higher than the 50% condition. The fast group showed no significant difference between the 33% and 50% conditions, which were both significantly lower than the 25% duty cycle. Significant differences were found among each of the duty cycles for the mixed twitch group, with decreasing duty cycle consistently increasing moment maintenance.

E. Carousel Stimulation Outcomes

Carousel stimulation trials were performed using the T = 1 second stimulation period and the lowest duty cycle possible based on the cuff's selectivity. In cases where multiple groups of low overlapping contacts could be identified within a single cuff, contacts for the paradigm were chosen and interspersed based on twitch contraction times and muscle types, in accordance with the significant differences indicated above. MG motor units and those with slow twitch contraction properties were preferentially included over LG and TP motor units and those that showed purely fast twitch contraction responses. Table 1 summarizes the involved contact characteristics and resulting outcome measures (moment ripple, moment overshoot, and T50) for constant, open-loop carousel, and closed-loop carousel stimulation trials for three groups of contacts tested across three cuffs.

Figure 12 displays the raw data moment traces representative of each of these tests. All carousel attempts, both open- and closed-loop, showed prolonged moment maintenance for each group of MUPs over constant stimulation through the same contacts, as can be seen qualitatively in Figure 12 and quantitatively by the consistently higher T50 values in Table 1. This held true even in a "worst case" carousel scenario in which only two independent MUPs are available (Group A). Moment overshoot was decreased with closed-loop carousel compared with both open-loop and constant stimulation in all cases. Similarly, the large moment ripple seen with open-loop carousel was significantly ($p < 0.01$) reduced by closed-loop control in all cases. In one case (Group A), moment feedback control reduced moment ripple to the point of no significant difference with that of constant stimulation.

IV. Discussion

A. Stimulation Period

The extent and time-course of fatigue were significantly influenced by stimulation period. Cyclic stimulation results reveal that a period of one second maintains significantly higher mean moments than longer periods after the same amount of contraction time. Higher mean moments indicate that the shorter contractions led to less overall moment decline and decline at a slower rate. These results suggest that decreasing the amount of time a motor unit must contract before allowed to rest significantly improves the maintenance of moment output. This is in

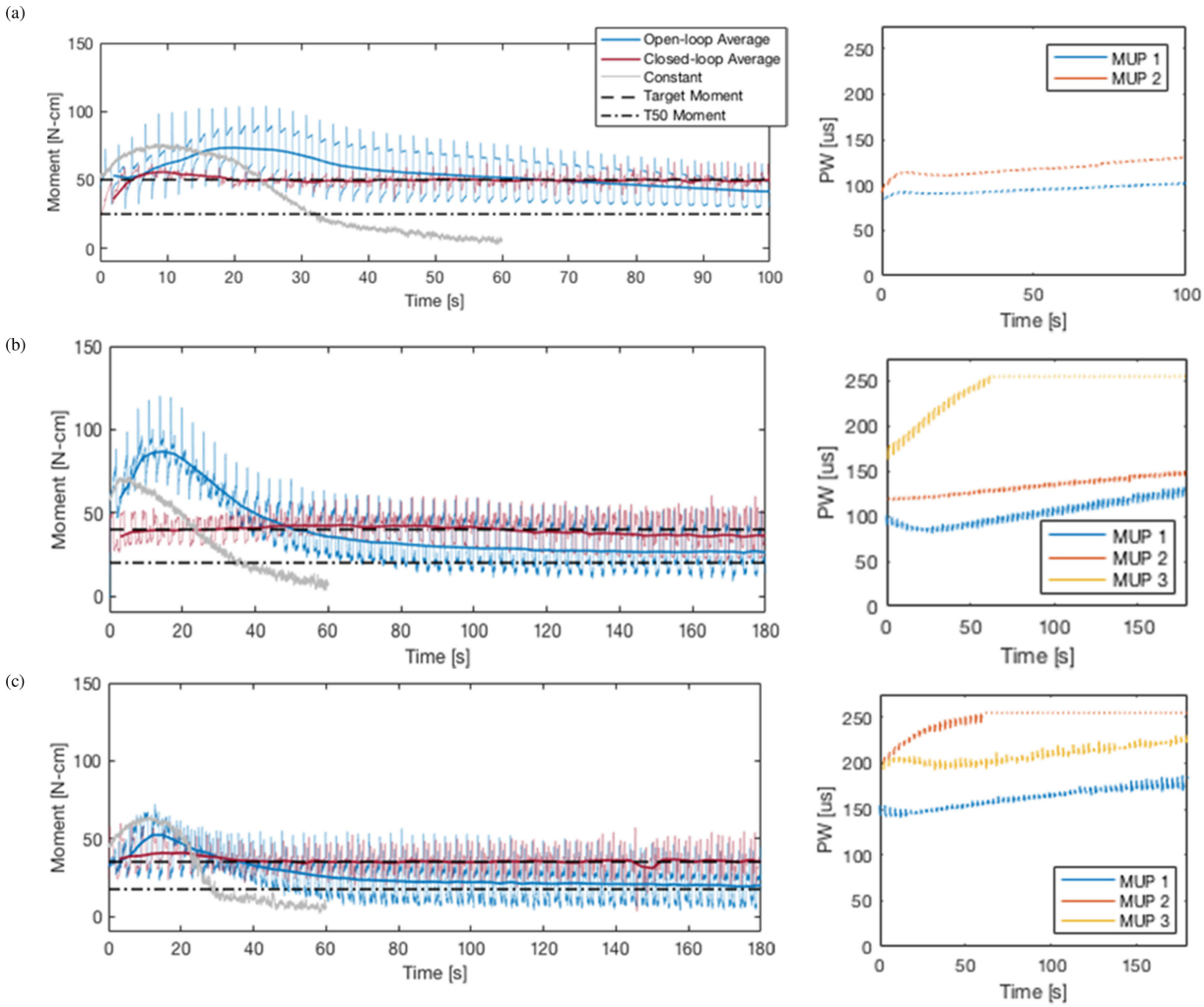

Fig. 12. Performance of ASPs compared to constant and open-loop stimulation for three different groups of contacts. (a) c = 2, T = 1, target moment = 50 N-cm (b) c = 3, T = 1, target = 40 N-cm (c) c = 3, T = 1, target = 40 N-cm.(Left) Raw ASP moment traces are shown in faded blue and red traces for open and closed-loop trials respectively. Mean moment traces averaged over each full cycle through contacts are overlaid as darker solid lines. (Right) Feedback controller PW output to each contact during closed-loop carousel trials.

accordance with other studies that have measured muscle force fatigue and recovery in response to intermittent stimulation of different lengths [33], [34]. These studies each concluded that decreased stimulation periods resulted in greater tension after 60 seconds but did not test any periods shorter than five seconds or include an analysis of within-contraction moment decline.

What makes the results of our study somewhat surprising is the short stimulation "on" times in turn cause the rest periods that follow to also be shorter in this setup (since 50% duty cycles were used for each T condition). This suggests that preventing the onset of moment decline is more strategic than allowing longer periods of recovery. This is supported by recovery time courses determined theoretically and experimentally in other studies [35], [36]. In one study, four muscles with different known muscle fiber type distributions in healthy human participants were subjected to one minute of fatiguing contractions. Recovery times to reach the same initial moment output consistently exceeded the one-minute fatigue time, with some muscles requiring over six minutes just to recover the prior maximum voluntary contraction [35]. Similarly, optimization of a three-compartment model of muscle fatigue and recovery consistently found lower time constants for fatigue than recovery in each muscle tested. Based on the ratio of fatigue rate and recovery rate parameters, authors concluded that muscles fatigue 10 to 15 times faster than they can recover [36].

Short stimulation periods that allow for more rapid rotation through contracting motor units may more closely resemble the physiologic asynchrony of natural muscle contraction by removing some of the synchrony that results from currently used constant stimulation. This rapid switch between on and off muscle states may also aid in enabling adequate blood flow to the muscles. Whereas long stretches of muscle contraction can cause a decrease in muscle perfusion or even ischemia and thus result in a switch from aerobic to anaerobic mechanisms [37], short bursts of contraction may enable rest periods to be reached and metabolites to replenish before anaerobic metabolism becomes necessary. This notion could explain the higher deltas seen for the T = 5 and T = 10 seconds, as prolonged contraction may have led to anaerobic metabolism and the rapid loss of muscle output within a single period.

There is a physiological lower limit to effective stimulation periods during prolonged static contractions, though, as the muscle fibers must be able to fully relax in its rest period before stimulation causes another contraction. Following the trend of lower periods proving superior, the present study attempted to use stimulation periods of 0.3 and 0.5 seconds through a few randomly chosen contacts. Results of these tests revealed that at a 50% duty cycle, moment output ceased to return to baseline as the trial went on. Thus, the muscle fibers were unable to consistently and fully relax during off periods at the highest duty cycle with these very short stimulation periods. Studies have found that relaxation time from tetany significantly increases as a muscle further fatigues [38]. While 300–500 ms of rest may initially be adequate for full relaxation, these times can become insufficient once fatigue processes begin. The cyclic stimulation experiments were thus limited to a minimum of T = 1 second, since the MUPs activated by all tested contacts were able to fully relax such that moment output returned to baseline during each rest period under this condition. During functional applications, this lower limit is specific to prolonged static contractions, such as knee extension during standing, and when a high duty cycle is necessary due to a low number of synergistic contacts available. In more repetitive movements like walking, lower stimulation periods could be used as a different MUP could produce the desired movement each step, reducing the duty cycle of each MUP well below 50%.

It is possible that each stimulation period tested would eventually level off to similar values with prolonged trial lengths, once fast twitch MUPs fatigue and the only moment produced is from the remaining slow twitch fibers. This study did not investigate trials longer than one minute of active contraction since the primary goal was to prolong high levels of MUP output from the onset of stimulation. One minute of active stimulation was sufficient to realize significant differences among the stimulation periods chosen, so any further changes in moment output beyond that point were considered outside the scope of this study.

B. Muscle Identification and Duty Cycle

This study confirmed previous findings that reduced duty cycles prolong muscle output for the same amount of active stimulation time [39]. Significant differences found when grouping the duty cycle results based on muscle predicted from moment space trajectory enable the MUPs that best prolong moment output to be quickly identified. Medial gastrocnemius fibers have been shown here to maintain moment output at higher duty cycles than tibialis posterior fibers. This finding is supported by the relative muscle fiber type distributions of these two muscles. Histological analyses of the cat hindlimb have revealed approximately 56% of MG motor units to be slow or fatigue resistant [40], while a majority of TP motor units are fast fatigable [41]. Lateral gastrocnemius/soleus fibers were found to perform well at a low 25% duty cycle and significantly worse at a 50% duty cycle, but as a group remain ambiguous at the 33% condition. This is likely due to grouping of lateral gastrocnemius motor units, which have a higher proportion of fast fatigable fibers [40], [42], and soleus motor units, which are predominately slow twitch [43]. Distinguishing these muscles from each other through moment space analyses alone is quite difficult as they share strikingly similar trajectories. Better results may be obtained through manual muscle tests and EMG in addition to moment spaces to reliably separate out muscle types. As fiber type distribution across various muscles is well documented in both animals and humans, results from the present study can be easily combined with already available knowledge to pick appropriate paradigm parameters in clinical applications.

C. Motor Unit Type Identification and Duty Cycle

The ability to determine muscle fiber type through twitch contraction times evoked by direct neural stimulation has previously been demonstrated [31], [40]. These earlier studies were performed on isolated muscle of the feline hindlimb and further confirmed through histology. The present study, to the authors' knowledge, is the first to demonstrate that such distinctions can be achieved with neural stimulation of intact muscle through a single nerve cuff and to directly correlate that classification to parameters affecting moment maintenance. Though histologic analysis of motor unit pools was not performed here for confirmation, clear and significant differences in cyclic stimulation outcomes show that a functional distinction can be made based on twitch contraction times in this manner. MUPs classified as slow twitch based on twitch contraction time showed no statistical significance between 25% and 33% duty cycles, while purely fast and mixed twitch motor units did show a significant decrease. This indicates that slowly fatiguing fibers can be identified via twitch responses and can be interspersed more frequently within a paradigm. More frequent stimulation of slow twitch fibers would allow longer rest periods for faster fatiguing fibers without compromising the slow twitch fibers' own moment output.

D. Carousel Stimulation – Open vs Closed-Loop Control

Carousel stimulation with appropriately chosen MUPs and stimulation parameters consistently maintained moment for longer durations than constant stimulation (Figure 12, Table I). Though joint moment results are specific to skeletal muscle applications, these stimulation strategies could benefit any neural prosthesis that requires long or continuous contractions, such as in cardiomyoplasty or diaphragm pacing.

Despite the use of T = 1 s for low within contraction variation in moment, open loop carousel stimulation still results in a high initial overshoot of the desired moment and a large amount of moment ripple (Table I). Motor units involved in these paradigms still potentiate and eventually fatigue at various rates, which causes significant changes in moment when switching from one contact to the next resulting in the observed moment ripple. Moment ripple was significantly ($p < 0.01$) reduced with implementation of a moment-matching controller. The amount of ripple in PID control appears correlated with the number of contacts in the paradigm. PID controlled ripple in the $c = 2$ condition was significantly lower than that of the $c = 3$ conditions, though this may be due to the added difficulty in

TABLE I
A SUMMARY OF CONSTANT VS OPEN- AND CLOSED-LOOP CAROUSEL TRIALS

Group	c	Contact Characteristics		Stimulation	Outcome Measures		
		Muscle	*Fiber Type (Twitch Time)*		*Moment Ripple (%)*	*Moment Overshoot (% Target)*	*T50 (s)*
A	2	MG	Slow (55 ms)	Constant	0.25 ± 0.23	0.53	30.78
				Open-loop Carousel	0.85 ± 0.06*	0.46	>100*
		LG/sol	Mixed (39/75 ms)	Closed-loop Carousel	0.32 ± 0.12∫∫	0.11	>100*
B	3	MG	Slow (59 ms)	Constant	0.25 ± 0.21	0.75	32.79
		LG/sol	Slow (65 ms)	Open-loop Carousel	1.24 ± 0.37*	1.17	69.01
		LG/sol	Mixed (41/89 ms)	Closed-loop Carousel	0.54 ± 0.16#∫∫	0.07	>180*
C	3	LG/sol	Slow (68 ms)	Constant	0.34 ± 0.27	0.61	27.59
		MG	Mixed (35/71 ms)	Open-loop Carousel	1.70 ± 0.61*	0.25	42.18
		MG	Mixed (42/70 ms)	Closed-loop Carousel	0.73 ± 0.17#∫∫	0.17	145.61

*T50 exceeded duration of trial
#Significantly greater ($p < 0.01$) than Constant Stun
∫∫Significantly less ($p < 0.01$) than Open-loop Stim
Moment ripple, moment overshoot, and T50 outcome measures are presented for three groups of MUPs activated with each paradigm. Increased T50 indicates prolonged joint moment maintenance. Decreased moment ripple indicates greater paradigm stability. Decreased moment overshoot indicates more consistent maintenance of target moment and reduced excess energy expenditure. Closed-loop carousel stimulation was found to outperform open-loop carousel and constant stimulation in each of these measures for all groups tested.

tuning more controllers. Minimizing ripple is important so that users will feel stable while using moment-prolonging paradigms during functional tasks such as standing. Though moment output may be high enough to maintain adequate knee extension in an open-loop carousel system, large amounts of ripple can create knee bouncing and make users feel uncomfortable and unsafe. Feedback control minimizes this and would enable users to more confidently rely on their activated muscles for support as opposed to compensating with other means, such as heavily supporting their weight through their arms on a walker. The PID controller also greatly reduces high overshoot of the desired moment seen with open-loop and constant stimulation, which saves energy expenditure for future use. This would enable neuroprosthesis users the opportunity to repeatedly perform actions, as they would not waste extraneous energy during a single repetition.

Although it has been shown here that reducing the duty cycle of each MUP does prolong joint moment output over constant stimulation, it will not do so indefinitely. PID control has the added benefit of recruiting more muscle fibers into the paradigm when the original fibers eventually fatigue. When fatigue does set in and the fibers originally activated in carousel stimulation cannot maintain the desired moment, PID control can increase the stimulus PW to recruit additional, yet-to-be fatigued fibers. This allows joint moment to be maintained for as long as possible. Cardiovascular benefits from stimulation-induced aerobic exercise will greatly increase from such a system that significantly prolongs the time users are able to stand, walk, cycle, or otherwise workout.

It should be noted that in two of the closed-loop carousel trials (Groups B and C), the feedback controller reached the stimulator's upper limit for one MUP after only a few carousel rotations. Closed-loop trials were the last tests performed in a given trial set. Though long rest periods were given to prevent effects of fatigue between each stimulation paradigm, it is possible that some muscle fibers were already exhausted and thus could not maintain target moment for long even at the highest stimulus. This may artificially inflate the moment ripple measurements calculated for closed-loop trials, as at least one MUP was too fatigued to match the output of the others. Even so, closed-loop carousel results still outperformed open-loop carousel in reducing moment ripple, and outperformed both constant and open-loop carousel in reducing moment overshoot and increasing time to T50. It is expected that when implemented with fully rested muscle fibers, improvements from feedback-controlled carousel would be even more pronounced.

The PID feedback controller implemented in this study utilized real-time isometric joint moment measurements from the JR3 load cell while the hindlimb was fixed in the stereotactic frame. This proved extremely effective in an experimental setting but would not suffice in real-world functional tasks where a person's limbs must be free to move. Furthermore, this controller only measured overall joint moment output, not contributions from each muscle group individually. In a carousel scheme where only one fiber group is active at a time, this is sufficient. However, more sophisticated patterns, such as carousel with ramp up and ramp down phases, may require multiple muscles to be activated to different degrees simultaneously. In these cases, it would be necessary to measure individual contributions from each activated group for precise control. Such a controller would need a new source of feedback and would require longer tuning and computational times.

V. CONCLUSION

Rotating activation of independent motor unit pools with advanced paradigms through a selective nerve cuff electrode prolongs joint moment output with neural stimulation. The success

and stability of these paradigms are greatly influenced by two stimulation waveform parameters: stimulation period and duty cycle of involved MUPs.

The present work has served to narrow this vast parameter space. A low stimulation period of T = 1 second best maintains moment while minimizing within-contraction variation and allowing for full relaxation at the highest duty cycle for all MUPs tested. Effective duty cycle varies by muscle and fiber type recruited by each contact on a selective nerve cuff. Some MUPs show no additional gain in joint moment output at duty cycles below 33%, while others require 25% or lower duty cycles for moment maintenance, supporting hypothesis I.

The present study then identified two strategies for quickly and reliably assessing a MUPs fatiguability. Muscle recruitment, either through manual muscle tests or moment space analyses, and predicted muscle fiber type identified via simple twitch responses, can both be readily determined with standard laboratory equipment. Both moment space trajectories and twitch contraction times were found to be reliable methods for classifying MUPs, as evident from the significant differences in allowable duty cycles amongst groups, supporting hypothesis II. The ability to obtain estimates of fiber type composition from simple and easily measured contractile properties enables informed incorporation of MUPs within advanced paradigms, ultimately leading to prolonged joint moment output.

Finally, this work has demonstrated the benefits of a moment-feedback controller for achieving balanced joint moment output from these different MUPs. Real-time joint moment feedback increased moment maintenance (T50) while reducing moment overshoot and ripple. Closed-loop stimulation consistently improved outcome measures compared to open-loop or constant stimulation through the same group of contacts, supporting hypothesis III.

Future work aims to translate these findings to human participants already implanted with selective nerve cuffs to prolong joint moments during functional tasks such as standing, stepping, and cycling. Prolonging moment output with neural stimulation systems will ultimately increase independence and improve clinical outcomes for recipients of motor system neuroprostheses.

Acknowledgment

The contents do not represent views of the U.S. Department of Veterans Affairs or the U.S. Government. Contribution from Lee Fischer, Ph.D., is also gratefully acknowledged.

References

[1] M. K. McDonnell *et al.*, "Electrically elicited fatigue test of the quadriceps femoris muscle," *Phys. Therapy*, vol. 67, no. 6, pp. 941–945, Jun. 1987.

[2] D. R. Sinacore, R. B. Jacobson, and A. Delitto, "Quadriceps femoris muscle resistance to fatigue using an electrically elicited fatigue test following intense endurance exercise training," *Phys. Therapy*, vol. 74, no. 10, pp. 930–939, Oct. 1994.

[3] E. Henneman, G. Somjen, and D. O. Carpenter, "Functional significance of cell size in spinal motoneurons," *J. Neurophysiol.*, vol. 28, pp. 560–580, 1964.

[4] E. Henneman, "Relation between size of neurons and their susceptibility to discharge," *Science*, vol. 126, no. 3287, pp. 1345–1347, Dec. 1957.

[5] Z. Lertmanorat, K. J. Gustafson, and D. M. Durand, "Electrode array for reversing the recruitment order of peripheral nerve stimulation: Experimental studies," *Ann. Biomed. Eng.*, vol. 34, no. 1, pp. 152–160, 2006.

[6] Z.-P. Fang and J. T. Mortimer, "A method to effect physiological recruitment order in electrically activated muscle," *IEEE Trans. Biomed. Eng.*, vol. 38, no. 2, pp. 175–179, Feb. 1991.

[7] Z.-P. Fang and J. T. Mortimer, "Selective activation of small motor axons by quasitrapezoidal current pulses," *IEEE Trans. Biomed. Eng.*, vol. 38, no. 2, pp. 168–174, Feb. 1991.

[8] C. S. Bickel, C. M. Gregory, and J. C. Dean, "Motor unit recruitment during neuromuscular electrical stimulation: A critical appraisal," *Eur. J. Appl. Physiol.*, vol. 111, no. 10, pp. 2399–2407, Oct. 2011.

[9] D. McDonnall, G. A. Clark, and R. A. Normann, "Interleaved, multisite electrical stimulation of cat sciatic nerve produces fatigue-resistant, ripple-free motor responses," *IEEE Trans. Neural Syst. Rehabil. Eng.*, vol. 12, no. 2, pp. 208–215, Jun. 2004.

[10] R. J. Downey *et al.*, "Comparing the induced muscle fatigue between asynchronous and synchronous electrical stimulation in able-bodied and spinal cord injured populations," *IEEE Trans. Neural Syst. Rehabil. Eng.*, vol. 23, no. 6, pp. 964–972, Nov. 2015.

[11] K. Yoshida and K. Horch, "Selective stimulation of peripheral nerve fibers using dual intrafascicular electrodes," *IEEE Trans. Biomed. Eng.*, vol. 40, no. 5, pp. 492–494, May 1993.

[12] U. Stanic *et al.*, "Multichannel electrical stimulation for correction of hemiplegic gait," *Scand. J. Rehabil. Med.*, vol. 20, no. 25, pp. 175–192, 1977.

[13] J. Petrofsky and C. Phillips, "Closed-loop control of movement of skeletal muscle," *CRC Crit. Rev. Biomed. Eng.*, vol. 13, no. 1, pp. 35–75, 1985.

[14] R. J. Triolo *et al.*, "Selectivity of intramuscular stimulating electrodes in the lower limbs," *J. Rehabil. Res. Develop.*, vol. 38, no. 5, pp. 533–544, 2001.

[15] M. D. Tarler and J. T. Mortimer, "Selective and independent activation of four motor fascicles using a four contact nerve-cuff electrode," *IEEE Trans. Neural Syst. Rehabil. Eng.*, vol. 12, no. 2, pp. 251–257, Jun. 2004.

[16] L. E. Fisher, D. J. Tyler, and R. J. Triolo, "Optimization of selective stimulation parameters for multi-contact electrodes," *J. Neuroeng. Rehabil.*, vol. 10, no. 25, 2013.

[17] L. E. Fisher *et al.*, "Standing after spinal cord injury with four-contact nerve-cuff electrodes for quadriceps stimulation," *IEEE Trans. Neural Syst. Rehabil. Eng.*, vol. 16, no. 5, pp. 473–478, 2008.

[18] M. A. Schiefer *et al.*, "Selective activation of the human tibial and common peroneal nerves with a flat interface nerve electrode," *J. Neural Eng.*, vol. 10, no. 5, 2014, Art. no. 056006.

[19] D. K. Leventhal and D. M. Durand, "Subfasicle stimulation selectivity with the flat interface nerve electrode," *Ann. Biomed. Eng.*, vol. 31, pp. 643–652, 2003.

[20] W. M. Grill and J. T. Mortimer, "Quantification of recruitment properties of multiple contact cuff electrodes," *IEEE Trans. Rehabil. Eng.*, vol. 4, no. 2, pp. 49–62, Jun. 1996.

[21] J. M. Hausdorff and W. K. Durfee, "Open-loop position control of the knee joint using electrical stimulation of the quadriceps and hamstrings," *Med. Biol. Eng. Comput.*, vol. 29, pp. 269–280, 1991.

[22] M. Ferrarin *et al.*, "Model-based control of FES-induced single joint movements," *IEEE Trans. Neural Syst. Rehabil. Eng.*, vol. 9, no. 3, pp. 245–257, Sep. 2001.

[23] D. J. Tyler and D. M. Durand, "Functionally selective peripheral nerve stimulation with a flat interface nerve electrode," *IEEE Trans. Neural Syst. Rehabil. Eng.*, vol. 10, no. 4, pp. 294–303, Dec. 2002.

[24] M. J. Freeberg *et al.*, "The design of and chronic tissue response to a composite nerve electrode with patterned stiffness," *J. Neural Eng.*, vol. 14, no. 3, Jun. 2017, Art. no. 036022.

[25] M. Freeberg *et al.*, "Chronic nerve health following implantation of nerve cuff electrodes designed for the proximal femoral nerve," *Neurology*, vol. 90, Apr. 2018, Art. no. S37.001.

[26] S. C. Trier *et al.*, "A modular external control unit for functional electrical stimulation," in *Proc. 6th Annu. Conf. Int. Functional Elect. Stimulation Soc.*, 2001, pp. 312–314.

[27] A. S. Gorgey *et al.*, "Effects of electrical stimulation parameters on fatigue in skeletal muscle," *J. Orthopaedic Sports Phys. Therapy*, vol. 684, no. 9, pp. 684–692, 2009.

[28] W. K. Durfee and K. E. MaClean, "Methods for estimating isometric recruitment curves of electrically stimulated muscle," *IEEE Trans. Biomed. Eng.*, vol. 36, no. 7, pp. 654–667, Jul. 1989.

[29] M. J. Freeberg, "Anatomically-versatile peripheral nerve electrodes preserve nerve health, recruit selectively, and stabilize quickly," Case Western Reserve Univ., Cleveland, OH, USA, 2018.
[30] T. Hamada *et al.*, "Postactivation potentiation, fiber type, and twitch contraction time in human knee extensor muscles," *J. Appl. Physiol.*, vol. 88, no. 6, pp. 2131–2137, Jun. 2000.
[31] R. M. Reinking, J. A. Stephens, and D. G. Stuart, "The motor units of cat medial gastrocnemius: Problem of their categorisation on the basis of mechanical properties," *Exp. Brain Res.*, vol. 23, no. 3, pp. 301–313, Sep. 1975.
[32] J. H. Lawrence, T. R. Nichols, and A. W. English, "Cat hindlimb muscles exert substantial torques outside the sagittal plane," *J. Neurophysiol.*, vol. 69, no. 1, pp. 282–285, Jan. 1993.
[33] Y. Giat, J. Mizrahi, and M. Levy, "A model of fatigue and recovery in paraplegic's quadriceps muscle subjected to intermittent FES," *J. Biomech. Eng.*, vol. 118, no. 3, pp. 357–366, 1996.
[34] M. Pournezam *et al.*, "Reduction of muscle fatigue in man by cyclical stimulation," *J. Biomed. Eng.*, vol. 10, no. 2, pp. 196–200, Apr. 1988.
[35] H. S. Milner-Brown, M. Mellenthin, and R. G. Miller, "Quantifying human muscle strength, endurance and fatigue A. Force and EMG measurements," *Arch. Phys. Med. Rehabil.*, vol. 67, pp. 530–535, 1986.
[36] L. A. Frey-Law, J. M. Looft, and J. Heitsman, "A three-compartment muscle fatigue model accurately predicts joint-specific maximum endurance times for sustained isometric tasks.," *J. Biomechanics*, vol. 45, no. 10, pp. 1803–1808, Jun. 2012.
[37] M. Gourdin and P. Dubois, "Impact of ischemia on cellular metabolism," in *Artery Bypass*. Rijeka, Croatia: InTech, 2013.
[38] J. Celichowski and E. Bichler, "The time course of the last contractions during incompletely fused tetani of motor units in rat skeletal muscle," *Acta Neurobiologiae Exp. (Wars).*, vol. 62, no. 1, pp. 7–17, 2002.
[39] J. Duchateau and K. Hainaut, "Electrical and mechanical failures during sustained and intermittent contractions in humans," *J. Appl. Physiol.*, vol. 58, no. 3, pp. 942–947, Mar. 1985.
[40] R. E. Burke *et al.*, "Physiological types and histochemical profiles in motor units of the cat gastrocnemius," *J. Physiol.*, vol. 234, no. 3, pp. 723–748, Nov. 1973.
[41] J. C. McDonagh *et al.*, "Tetrapartite classification of motor units of cat tibialis posterior," *J. Neurophysiol.*, vol. 44, no. 4, pp. 696–712, Oct. 1980.
[42] A. W. English and W. D. Letbetter, "A histochemical analysis of identified compartments of cat lateral gastrocnemius muscle," *Anatomical. Rec.*, vol. 204, no. 2, pp. 123–130, Oct. 1982.
[43] R. E. Burke *et al.*, "Motor units in cat soleus muscle: Physiological, histochemical and morphological characteristics," *J. Physiol.*, vol. 238, pp. 503–514, 1974.